10-28-2010

A Fish Out of Water: Gill and Skin Remodeling Promotes Osmo- and Ionoregulation in the Mangrove Killifish *Kryptolebias marmoratus*

Danielle M. LeBlanc
University of Guelph

Chris M. Wood
McMaster University

Douglas S. Fudge
Chapman University, fudge@chapman.edu

Patricia A. Wright
University of Guelph

Recommended Citation

LeBlanc DM, Wood CM, Fudge DS, and Wright PA (2010) A fish out of water: Gill and skin remodelling promotes osmo- and ionoregulation in the magrove killifish. *Physiological and Biochemical Zoology* 83: 932-49. DOI: 10.1086/656307

A Fish Out of Water: Gill and Skin Remodeling Promotes Osmo- and Ionoregulation in the Mangrove Killifish *Kryptolebias marmoratus*

A Fish Out of Water: Gill and Skin Remodeling Promotes Osmo- and Ionoregulation in the Mangrove Killifish *Kryptolebias marmoratus*

Danielle M. LeBlanc[1]
Chris M. Wood[2]
Douglas S. Fudge[1]
Patricia A. Wright[1,*]
[1]Department of Integrative Biology, University of Guelph, Guelph, Ontario N1G 2W1, Canada; [2]Department of Biology, McMaster University, Hamilton, Ontario L8S 4K1, Canada

Accepted 7/8/2010; Electronically Published 10/28/2010

ABSTRACT

The euryhaline, amphibious mangrove killifish *Kryptolebias marmoratus* is known to survive weeks out of water in moist environments. We tested the hypothesis that the skin is a site of osmo- and ionoregulation in *K. marmoratus*. We predicted that under terrestrial conditions, gill and skin remodeling would result in an enhanced role for skin and a diminished role for the gills in osmo- and ionoregulation. Fish were exposed to water—either freshwater (FW, 1‰) or hypersaline water (saltwater [SW], 45‰)—or air over a moist surface of FW or SW for 9 d and then recovered in water. When fish were emersed for 9 d, ^{22}Na and ^{3}H-H_2O were exchanged across the cutaneous surface. Homeostasis of whole-body Cl^- and water levels but not of Na^+ levels was maintained over 9 d in air. In air-exposed fish, there was a significant increase in the size of skin ionocytes (in SW), a decrease in the number of skin mucous cells (in SW), and an increase in the gill interlamellar cell mass relative to those of fish in water. Gill ionocytes were mostly embedded away from the external surface in air-exposed fish, but the number and size of ionocytes increased (in FW). Interestingly, skin ionocytes formed distinct clusters of 20–30 cells. The estimated number of ionocytes over the whole skin surface was comparable to that in the gills. Overall, the findings support the hypothesis that the skin is a site of osmo- and ionoregulation in *K. marmoratus* in aquatic and terrestrial environments. Reversible cellular and morphological changes to the skin and gills during air exposure probably enhanced the cutaneous contribution to ion and water balance.

* Corresponding author; e-mail: patwrigh@uoguelph.ca.

Physiological and Biochemical Zoology 83(6):932–949. 2010. 1522-2152/2010/8306-9159$15.00. DOI: 10.1086/656307

Introduction

In most fishes, the gills are the primary site of osmo- and ionoregulation (Evans et al. 2005). Gill ionocytes play a role in regulating the salt concentration of the internal environment of the fish with respect to the external environment (Marshall and Grosell 2006). If a fish leaves water (emersion), its gill lamellae collapse because of the surface tension at the air-water interface, which in turn results in a shutdown of regulatory processes (i.e., respiration, nitrogen excretion, and osmo- and ionoregulation) and ultimately leads to death (Sayer and Davenport 1991; Sayer 2005). Therefore, when amphibious fishes are out of water, they must be able to osmo- and ionoregulate via alternative routes, modify their gills to function in air (Graham 1973, 2006; Hughes and Munshi 1979; Randall et al. 1999), or be able to tolerate nonregulation (Sayer 2005).

The skin may be an important site of regulatory processes during air exposure. Most blood vessels are located in the dermis, but in some amphibious fishes, blood vessels penetrating the epidermis may enhance cutaneous respiration during emersion (see Graham 1997 for review; Zhang et al. 2003). The amphibious mangrove killifish *Kryptolebias marmoratus* (formerly *Rivulus marmoratus*) has an epidermal thickness ranging from 6 to 50 μm, and epidermal capillaries have been found within 1 μm of the skin surface, decreasing the diffusion distance between blood and the external environment (Grizzle and Thiyagarajah 1987). In this species, the cutaneous surface appears to be important in gas exchange (Ong et al. 2007) and NH_3 excretion (Frick and Wright 2002*b*; Litwiller et al. 2006). The FW swamp eel (*Synbranchus marmoratus*) also endures long periods of emersion in a damp environment and continues to take up ions (albeit at low rates) from the environment through the cutaneous surface (Stiffler et al. 1986). Similarly, in the marble goby (*Oxyeleotris marmorata*) and the mudskipper (*Periophthalmodon schlosseri*), Ca^{2+} influx (but not efflux) continued at low rates through the cutaneous surface when the fish were placed in air on wet filter paper saturated with seawater (SW; Fenwick and Lam 1988). Furthermore, Wilkie et al. (2007) determined that the ventral skin surface is an important site of exchange in the FW African lungfish (*Protopterus dolloi*) during prolonged terrestrial exposure. Cutaneous ionocytes have been identified in larvae and in some adult fishes (e.g., Marshall 1977; Nonette et al. 1979; Perry and Wood 1985; Ishimatsu et al. 1992; Sturla et al. 2001; Hsiao et al. 2007), but

it is not known whether these cells are remodeled during prolonged air exposure.

We examined osmo- and ionoregulation during air exposure in the amphibious and euryhaline mangrove killifish *K. marmoratus*. *Kryptolebias marmoratus* is a small, cyprynodontid, self-fertilizing, hermaphroditic fish native to southern Florida, Central America, and South America. *Kryptolebias marmoratus* is able to tolerate hypoxia (<1 mg L^{-1} O_2; Dunson and Dunson 1999), hydrogen sulfide (Abel et al. 1987), varying salinity (0‰–114‰; King et al. 1989; Taylor et al. 2008), and air exposure (>2 mo in air; Taylor 1990). In the mangrove habitat, abrupt changes in salinity may occur because of rainfall, the tidal cycle, and the season (Davis et al. 1990; Taylor et al. 2008). Emersion behavior in *K. marmoratus* has been well documented in the ecological literature (e.g., Davis et al. 1990; Taylor 2000; Taylor et al. 2008), but there is no information on how they osmo- or ionoregulate when emersed.

The gills of *K. marmoratus* are assumed to be nonfunctional in air because they are no longer irrigated with water, there are no buccal or opercular movements, and the operculum remains closed. Also, after 7 d in air, a reversible interlamellar cell mass (ILCM) develops in the gills of *K. marmoratus*, which embeds the lamellae and reduces gill surface area (Ong et al. 2007). A gill ILCM also develops in other species in response to environmental temperature, oxygen (*Carassius carassius*, *Carassius auratus*, *Gymnocypris prezewalskii*; Sollid et al. 2003, 2005; Matey et al. 2009; Mitrovic and Perry 2009), or developmental changes in gill structure (*Arapaima gigas*; Brauner et al. 2004). However, these species remain in water, and the gill ionocytes appear on the outer surface (water edge) of the gill epithelium (Brauner et al. 2004; Mitrovic and Perry 2009), suggesting a continued involvement of the gill in iono- and osmoregulation. We predicted that a similar scenario would not occur in *K. marmoratus*, given that the gills are emersed during terrestrial episodes.

How do amphibious euryhaline fish like the mangrove killifish osmoregulate on land? We tested the hypothesis that the skin is a site of osmo- and ionoregulation in *K. marmoratus*. If so, then the skin should contain ionocytes, and the morphometrics of these cells may be regulated in response to varying environments. We predicted that during air exposure, the gills (if functional) would have a reduced role in exchange with the external environment but whole-body ionoregulatory and osmoregulatory homeostasis would be maintained because of exchange of water and ions across the cutaneous surface. We also predicted that to prevent desiccation, mucous cells in the skin and gills would play a greater role in mucus production during air exposure.

To test the hypothesis, killifish were acclimated to either FW (1‰) or hypersaline SW (45‰) for at least 1 mo before experimentation. The salinities were chosen because *K. marmoratus* are exposed to a wide range of salinities (0‰–65‰) in their natural habitat (Davis et al. 1990; Frick and Wright 2002*a*; Taylor et al. 2008). After the acclimation period, the fish were separated into three groups: (i) control (water), (ii) air exposure, and (iii) recovery. Air-exposed fish were placed on a moist surface in contact with either FW or SW for 9 d. Water and ion efflux rates were determined by use of ^{3}H-H_2O and ^{22}Na. Whole-body Na^+, Cl^-, and water contents were also measured. In the skin and gills, ionocytes were identified by means of a vital mitochondrial stain (2-(4-dimethylaminostyryl)-1-ethylpyridinium iodide; DASPEI) and immunohistochemistry for Na^+, K^+-ATPase (NKA), and periodic acid–Schiff (PAS) staining was used to identify mucous cells.

Material and Methods

Experimental Animals

Adult, hermaphroditic mangrove killifish *Kryptolebias marmoratus* Poey (formerly *Rivulus marmoratus*) at least 1 yr of age and weighing between 0.06 and 0.14 g were used in these experiments. Mangrove killifish were obtained from a breeding colony in the Hagen Aqualab at the University of Guelph, Ontario. The fish were held in individual containers (120 mL) within an environmental chamber mimicking average conditions in their natural environment (25°C, 16‰, pH 8, 12L : 12D cycle). Fish were held in artificial seawater made from tap water treated by reverse osmosis and Crystal Sea Marinemix (Marine Enterprises International, Baltimore). The water in each container was changed once per week, and the fish were fed 1 mL of concentrated live *Artemia* mixed with seawater three times a week.

Experimental Protocol

Two experiments were conducted. The first examined ion and water flux, and the second examined gill and skin remodeling during prolonged air exposure.

Experiment 1: Ion and Water Flux. Fish were transferred to FW (1‰) or hypersaline SW (45‰) for at least 1 mo before experimentation. At the start of the experiment, the fish were divided into four groups: (1) SW fish in water (control group), $N = 11$; (2) SW fish in air, $N = 8$; (3) FW fish in water (control group), $N = 10$; and (4) FW fish in air, $N = 8$. Fish in groups 1 and 3 were placed in individual containers filled with 20 mL of the appropriate medium (SW or FW) for 7 d. Air-exposed fish in groups 2 and 4 were placed in individual mesh-bottomed containers (120 mL) that were placed directly in contact with the surface of 20 mL of water (SW or FW) for 7 d. The water kept the mesh wet but never rose above it so as to prevent the fish from immersing their gills. Therefore, air exposure in this study is defined as the condition in which fish are sitting in air but in contact with water in a moist environment. This accurately reflects conditions killifish experience in the wild.

On the seventh day, fish in water (groups 1 and 3) were placed together with other fish from their respective groups in a 50-mL beaker containing 20 mL of the appropriate medium supplemented with 1 μCi mL^{-1} × ^{3}H-H_2O. On the seventh day of air exposure, the fish in groups 2 and 4 were placed together with other fish from their respective experimental groups in a mesh-bottomed container sitting in contact with 20 mL of the appropriate medium supplemented with 1 μCi

mL^{-1} × ^{3}H-H_2O. The fish were left overnight to absorb ^{3}H-H_2O and equilibrate with the external bath. In their natural habitat, killifish are often crowded together in crab burrows and rotting logs; therefore, crowding stress should not have greatly affected the results of this experiment (Taylor et al. 2008). Also, all groups experienced similar crowding. Approximately 12 h later, the fish in water were quickly rinsed, and each was placed in 20 mL of water without radioisotope. Similarly, fish in air were rinsed and placed in a mesh-bottomed container in contact with 20 mL of water. Water samples (5 mL) were taken from each container every 30 min for 10 h, and the volume was replaced with 5 mL of water after each sampling.

On completion of the ^{3}H-H_2O efflux period, the fish were weighed and returned to either water or air, as appropriate. These same fish were then used to measure ^{22}Na flux because the number of specimens available for study was very limited. On the eighth day, the fish were placed together in or in contact with the appropriate medium (as above). SW fish were exposed to 4 μCi mL^{-1} × ^{22}Na, whereas the FW fish were exposed to 0.4 μCi mL^{-1} × ^{22}Na. The fish were left overnight to absorb ^{22}Na from the water.

Approximately 12 h later and on the ninth day, fish were quickly rinsed in water without radioisotope, placed in a plastic vial (20 mL), and measured for total body ^{22}Na counts in a gamma counter (see below). Fish were counted for 1 min and then placed in individual experimental chambers in or in contact with 20 mL of water (as above). For SW fish, water samples (5 mL) were collected every 15 min for 3 h. For FW fish, water samples (5 mL) were collected every 30 min for 6 h. Sampling times were chosen on the basis of preliminary experiments that demonstrated that ^{22}Na washout occurred faster in the SW- than in the FW-acclimated fish. After each 5-mL water sample was removed, the volume was replaced with 5 mL of new water.

On completion of ^{22}Na efflux measurements, each fish was placed in a vial, and whole-body ^{22}Na counts were measured as described above. The fish were euthanized via cephalic blow, and body mass was recorded. During this experiment, handling may have resulted in high levels of stress in the fish. However, the experiment was arranged to minimize stress to the fish and to handle the fish equally in order to equalize stress. Also, the killifish used in this experiment were handled at least once a week for container cleanings, which may have desensitized them to some handling stress.

Experiment 2: Cell Composition of the Skin and Gills. Fish were transferred to FW (1‰) or hypersaline SW (45‰) for at least 1 mo before experimentation. At the start of the experiment, the fish were divided into six groups: (1) SW fish in water (control group), $N = 7$; (2) SW fish in air, $N = 8$; (3) SW fish in air and then recovered in water, $N = 8$; (4) FW fish in water (control group), $N = 8$; (5) FW fish in air, $N = 8$; and (6) FW fish in air and then recovered in water, $N = 7$. Fish in groups 1 and 4 were placed in individual containers filled with 20 mL of the appropriate medium (SW or FW) for 9 d. Fish in groups 2, 3, 5, and 6 were exposed to air for 9 d in individual mesh-bottomed containers (120 mL) that were placed in contact with the surface of a 20 mL pool of water (SW or FW). After 9 d in air, fish in the recovery condition (groups 3 and 6) were immersed in water (20 mL of either SW or FW, as appropriate) for 7 d.

On the ninth morning in water or air and the seventh day of recovery, the fish were placed together either in or above a 350-μM solution of DASPEI (Sigma-Aldrich, Oakville, Ontario) made with either SW or FW, depending on the group. DASPEI is a vital probe that accumulates in mitochondria, allowing for the detection and identification of ionocytes (also known as mitochondria-rich cells [MRCs]). DASPEI is a highly specific stain with low toxicity, and it has been used to identify ionocytes in live tilapia embryos without any indication of side effects (Bereiter-Hahn 1976; Hiroi et al. 1999). After an incubation period of at least 3 h, fish were lightly anesthetized with 2-phenoxy-ethanol (2-PE; 1.2 mL L^{-1}), rinsed in DASPEI-free water, and then imaged. The fish were placed on their dorsal surface on a thin sponge held down on a microscope slide with white petroleum jelly (Life Brand, Toronto). A coverslip was placed over the fish to restrict movement. The ventral surface of the fish was examined with a Nikon Eclipse 90i epifluorescent microscope (hereafter referred to as "the microscope"; Nikon Instruments, Melville, NY). The microscope was fitted with two cameras (a QImaging Retiga Exi and a QImaging QI Cam, QImaging, Surrey, British Columbia), and images were captured with the Nikon Imaging Software–Elements: Advanced Research program (NIS-Elements AR; Nikon Instruments). Immediately after imaging, the fish were euthanized with a lethal dose of 2-PE (2 mL L^{-1}) and weighed. The fish were fixed in 10% neutral buffered formalin for 24 h at 4°C, decalcified (1 h) with Surgipath Decalcifier II (Medical Industries, Richmond, IL), and preserved in 70% ethanol at 4°C before dissection and histological processing. Tissue was embedded in paraffin and sectioned at 4 μm.

Analysis

Radioactivity

To each 5-mL water sample containing ^{3}H-H_2O, 10 mL of aqueous counting scintillant (Amersham, Oakville, Ontario) was added, and the sample was then mixed and left in the dark (2 h) before beta radioactivity was measured with a Tri-Carb 2900TR liquid scintillation analyzer (Perkin Elmer, Waltham, MA). Each sample was counted for 5 min. Internal standardization tests demonstrated that quench was constant, so no correction was applied. The starting counts in the fish were estimated by multiplying the average percent body water by the mass of each fish and then multiplying this value (in mL) by the counts per minute per mL of the loading water. Water samples containing ^{22}Na as well as live fish were measured for gamma radioactivity using a Wallac Wizard 3 automatic gamma counter (Perkin Elmer). Each sample was counted for 5 min.

Efflux Calculations

The unidirectional efflux rate was determined by the rate of loss of radioisotope from the fish to the water. Unidirectional efflux rates (J_{out}) for Na^+ in μmol g^{-1} h^{-1} and for water in mL g^{-1} h^{-1} were then calculated with the following formula (see Wood and Laurent 2003):

$$J_{out} = \frac{K \times \sum_z \times F}{W},$$

where K is the rate constant of the amount of radioisotopic washout per hour, $\sum_z$ is the total measured internal pool of Na^+ or water (in μmol g^{-1} or mL g^{-1}, respectively), F is the fractional labeling of that pool, and W is body weight (g). Note that K was measured for each individual fish in each treatment, separately for each radioisotope, by fitting an exponential regression line to the loss of counts to the water against time. On the basis of preliminary experiments and earlier experience with other killifish (Wood and Laurent 2003), F was taken as 0.95 for ^{22}Na and 1.0 for ^3H-H_2O. Fractional labeling of the internal Na^+ and water pools was complete after 12 h, and individual values varied by less than 5%.

Whole-Body Na^+, Cl^- Content

The fish were euthanized via cephalic blow, weighed, and then placed in 1 mL of 1 N HNO_3 at 68°C for 48 h. The homogenate was mixed periodically. After 48 h, the digested material was cooled and centrifuged at 500 *g* for 5 min. The supernatant was diluted 10 times, and the Na^+ level of the solution was determined with atomic absorption spectrophotometry (Varian Australia Model 220FS, Mississauga, Ontario). Whole-body Cl^- content was determined with a colorimetric mercuric thiocyanate assay modified from Zall et al. (1956).

Body Water Content

Twenty-four fish acclimated to FW (1‰) or SW (45‰) for at least 1 mo before experimentation were used to determine percent body water. There were four treatment groups (in all cases $N = 6$): SW fish in water, SW fish in air, FW fish in water, and FW fish in air. To determine body water content, euthanized fish were blotted in a standardized fashion, then weighed and placed in a drying oven (50°C) for at least 3 d until constant mass was achieved. The formula [(wet mass − dry mass)/wet mass] × 100 was used to calculate body water content in fish that spent 9 d in either water or air.

Immunofluorescent Staining for NKA

To identify and quantify ionocytes in the skin and gills, NKA was localized with the α-5 antibody (mouse antichicken NKA) developed by D. M. Fambrough (Johns Hopkins University, Baltimore). Thin sections (4 μm) of skin and gills were deparaffinized in xylene (2 × 3 min), rehydrated in 100% ethanol (2 × 2 min), and allowed to air-dry before a hydrophobic barrier (PAP pen; Sigma-Aldrich) was applied around the sections. Once the barrier had dried around the sections, the slides were rinsed in phosphate-buffered saline (PBS, 3 × 5 min) and incubated for 1 h with 0.01% bovine serum albumin (BSA) and 5% normal goat serum (NGS) in PBS. The slides were left overnight at 4°C with the primary antibody (α-5, 1 : 50 dilution) in a buffer solution of 1 × PBS containing 0.05 mg mL^{-1} BSA, 0.05 mg mL^{-1} thyroglobulin, 2.5 mg mL^{-1} sodium azide, and 20 mg mL^{-1} ethylenediaminetetraacetic acid. The next day, the slides were rinsed in PBS (3 × 5 min), incubated for 1 h in the secondary antibody (Alexa fluor 488 goat antimouse IgG [H+L], 1 : 400 dilution; Invitrogen, Burlington, Ontario) in the buffer solution and rinsed again in PBS (3 × 5 min) before being mounted with a 1 : 1 glycerol : PBS solution and sealed with clear nail polish. The slides were visualized with the microscope, and images were captured with NIS-Elements AR. To determine the degree of nonspecific staining and autofluorescence, negative controls were used. On negative-control slides, either the primary and secondary antibodies or only the secondary antibody were left out of the buffer solution. All other steps remained the same. The negative controls demonstrated that there was no autofluorescence or nonspecific staining in the skin and gills. The spinal cord, liver, kidney, and gut fluoresced because of a higher concentration of NKA in those tissues (Clendenon et al. 1978; Fuentes et al. 1997; Sherwani and Parwez 2008).

Light Microscopy

Slides were stained with PAS to allow for identification of mucous cells in the tissue sections. Sections were examined on the microscope, and images were collected as above.

4′, 6-Diamidino-2-Phenylindole Staining

To ensure that DASPEI was specifically staining cells, DAPI (4′, 6-diamidino-2-phenylindole) was used in combination with DASPEI to identify nuclei in the cells. DAPI binds DNA and fluoresces under ultraviolet light, allowing for the detection and identification of nuclei (Kapuściński and Szer 1979). Live fish ($N = 3$) were incubated in 10 mL of a 350-μmol L^{-1} DASPEI solution (made with brackish water, 15‰ salinity) for at least 2 h before being euthanized with 2-PE (2 mL L^{-1}). DAPI was added to 10 mL of DASPEI solution for a final concentration of 0.182 μmol L^{-1}. Euthanized fish were returned to the DASPEI/DAPI solution for 1 h. The fish were then removed from the solution, placed on their dorsal surface, as above, and imaged with the microscope.

Counting and Measuring NKA-Labeled and Mucous Cells

All cell counts, cross-sectional area measurements, and gill morphometrics were performed with NIS-Elements AR by means of a coding system to ensure the experimenter was blind to the treatment. Also, cells were numbered during the counting pro-

cess and then chosen for cross-sectional area measurements via random-number selection in Microsoft Excel.

Skin. The cell counts of DASPEI images were performed at three sites along the ventral surface: (1) directly between the pectoral fins, (2) directly below the pectoral fins (midway along the body), and (3) 4 mm below the pectoral fins. At each site, the cross-sectional areas of 15 cells were determined in three 0.0625-mm^2 fields (5 cells × 3 fields = 15 cells $site^{-1}$ × 3 sites = 45 cells total $fish^{-1}$).

The NKA-labeled and PAS-stained images were of the skin in cross-section (the cross-sections were made directly behind the pectoral fins). The following protocol was performed separately for each staining technique. The circumference of each fish was divided into four equal sections; dorsal, ventral, and left and right lateral sides. The cross-sectional areas of two cells per section (8 cells $fish^{-1}$) were measured. Although data were collected separately for four sections, data from cell counts and cross-sectional area measurements were later combined for NKA-labeled cells and mucous-cell cross-sectional area measurements (but not mucous-cell counts) because there were no significant differences between sections.

Gills. Cell counts and area measurements were performed on four gill filaments per fish. The filaments were randomly selected by numbering all entire (undamaged) filaments in a section and randomly generating numbers in Microsoft Excel. In the NKA-labeled gills, the NKA cells found in 10 interlamellar spaces (ILSs) and on the lamella were counted separately (giving a count of the number of NKA cells per ILS). The cross-sectional areas of three NKA cells per filament were measured.

While we thoroughly examined the filaments, lamellae, and ILSs for mucous cells, they were very sparse (indeed none were found in some fish), and therefore no data have been presented. Gill morphometry measurements included lamellar length, lamellar width, and ILCM height, as previously described (Ong et al. 2007).

Cell-Cluster Analysis

In examinations of fish stained with DASPEI, it became apparent that the cells on the ventral surface of FW- and SW-acclimated fish were clustered. In SW fish, the clusters were examined at the same three sites imaged after DASPEI staining (see above). At each of the three sites, measurements of the areas of the clusters and the distance between adjacent clusters were taken, along with the number of cells in each cluster. The area of a cluster was measured by drawing a circular shape around the cluster, with cells on the outer edge as guides. The distance between the clusters was measured conservatively by taking the distance between the two closest cells in neighboring clusters.

Number of Ionocytes in the Skin versus the Gills

The number of skin ionocytes in the whole fish was estimated from the NKA-positive cell counts in 4-μm whole-body sections. The average diameter of these cells was ~10 μm. To determine the best approach for estimating the number of NKA-positive cells in the skin from these cell counts, we created a simulated two-dimensional (2D) fish skin in which a finite number of 10-μm-diameter cells were randomly placed on a grid with an area of 100,000 μm^2 and an average intercell spacing of about 20 μm, which is similar to the spacing on our fish. We measured the average rate of cells intersected by 40 randomly placed 4-μm slices. From these measurements, we calculated a cell encounter rate per 100 μm of linear distance that we took as characteristic for the density of cells in two dimensions (in units of cells μm^{-2}). To calculate the density of cells on our real fish, we multiplied the 2D density of cells in the simulation by the ratio of the linear encounter rate for the fish to the linear encounter rate in the simulation. The linear encounter rate for each fish was determined by taking the number of cells in a 4-μm slice of the total fish body and dividing by the circumference of the fish. Cell density values were then multiplied by the total surface area of the fish to estimate the total number of cells. Fish skin area for 10 fish was estimated by modeling each fish as two half cones (mean surface area = 59 mm^2).

To estimate the number of ionocytes in the whole gill, the average number of NKA-positive cells per gill filament (very few cells were found in the lamellae) was calculated in the plane of the 4-μm sections. The depth of the filament was determined in micrometers from a separate set of gill micrographs perpendicular to the plane of the original micrographs. Filament depth was 67.5 ± 13.2 μm ($N = 3$) for SW fish in water and 58.6 ± 5.3 μm ($N = 3$) for FW fish in water. To estimate the total number of ionocytes in the gills, the average filament depth (above) was divided by the average diameter of an ionocyte (SW fish in water = 14.6 ± 5.1 μm; FW fish in water = 11.4 ± 2.5 μm). This ratio was then multiplied by the number of ionocytes per gill filament (measured individually in each fish), the average number of gill filaments per hemibranch (36.1 ± 1.3), the number of hemibranchs per arch (2), and the number of arches per fish (4).

Statistical Analysis

All data are presented as means ± SEM. For measures in experiment 1 (^3H-H_2O and Na^+ efflux rates, whole-body ions, and whole-body water content), individual 2 × 2 factorial ANOVAs were conducted. For some measures in experiment 2 (ionocyte counts and area measurements in the gills and gill morphometric analyses), individual 2 × 3 factorial ANOVAs were also conducted. For DASPEI staining, individual 2 × 3 × 3 mixed-model ANOVAs were conducted. For NKA and mucous cell counts and cross-sectional area measurements, individual 2 × 3 × 4 mixed-model ANOVAs were conducted. All analyses were done with SPSS, version 13.0, and $P \leq 0.05$ was considered significant. After

a significant result, simple main-effects tests were conducted with a Bonferroni adjustment.

Results

Water and Ions

In both water and air, FW fish had significantly higher water efflux rates than SW fish, a difference of two- to threefold (Fig. 1*A*). Air-exposed FW fish had significantly higher water efflux rates relative to FW fish in water (Fig. 1*A*). In contrast, SW air-exposed fish had significantly lower water efflux rates than SW fish in water (Fig. 1*A*).

FW fish had much lower Na^+ efflux rates than SW fish in both water and air, a difference of approximately 16-fold, but air exposure had no effect on Na^+ efflux rates at either salinity (Fig. 1*B*). Whole-body Na^+ concentration was significantly higher in SW fish than in FW fish (Fig. 1*C*). Air-exposed FW fish had slightly (but significantly) lower Na^+ concentrations than FW fish in water (Fig. 1*C*). Air-exposed SW fish had significantly higher whole-body Na^+ concentrations than SW fish in water (Fig. 1*C*). Whole-body Cl^- concentrations ($FW_{water} = 66.0 \pm 6.8$ μmol g^{-1}; $FW_{air} = 67.5 \pm 2.8$ μmol g^{-1}; $SW_{water} = 68.1 \pm 4.7$ μmol g^{-1}; $SW_{air} = 66.1 \pm 4.2$ μmol g^{-1}) and percent body water content ($FW_{water} = 76.7 \pm 0.2$; $FW_{air} = 76.4 \pm 0.4$; $SW_{water} = 76.7 \pm 0.2$; $SW_{air} = 76.5 \pm 0.2$) were not significantly different between any of the groups.

MRCs in the Skin

The mitochondrial marker DASPEI revealed the presence of two "types" of cells in the skin. The cells were distinguished by shape and pattern of illumination. There were oval cells that were stained strongly and uniformly throughout the whole cell (Fig. 2*A*, 2*B*) and round cells that were stained around the edges and looked like doughnuts (Fig. 2*A*). The round cells were primarily found in the FW fish. To ensure that the oval and round stained objects were indeed cells and not nonspecific staining (or staining artifacts), DAPI (a nuclear stain) revealed that nuclei were present in both cell types (Fig. 2*C*, 2*D*). In the images, a nucleus does not appear in every cell. However, this is probably because the dye was unable to penetrate through some layers of the skin. Also, some nuclei do not appear to be in DASPEI-positive cells. This is because DAPI is not specific to MRCs and other skin cells bound with DAPI.

In general, the number of oval MRCs in the skin of FW and SW fish was similar; however, $SW_{recovery} > FW_{recovery}$ and $FW_{recovery} < FW_{water}$ and FW_{air} (Fig. 2*E*). In all groups, oval MRCs were significantly larger in SW fish than in FW fish (Fig. 2*F*). Within the SW treatment, MRCs were significantly larger in air-exposed fish than in fish in water and recovery fish. Also, oval MRCs were significantly larger in SW recovery fish relative to SW fish in water (Fig. 2*F*).

In contrast to oval cells, the number of round MRCs was greater in FW fish than in SW fish (Fig. 2*G*). The cross-sectional area of round MRCs in FW fish was not affected by treatment ($FW_{water} = 227 \pm 7$ μm^2, $FW_{air} = 193 \pm 5$ μm^2, $FW_{recovery} = 219 \pm 12$ μm^2). There were insufficient numbers of round MRCs in SW fish to analyze data.

NKA-Rich Cells in the Skin

In whole-body cross-sections, immunohistochemistry of NKA showed a strong signal in intestine, kidney, spinal column, and skin (Fig. 3*A*). At higher magnification, NKA-rich cells in the skin were observed on the epidermal surface close to the external environment (Fig. 3*B*). The SW fish had significantly more NKA cells than the FW fish (Fig. 3*C*). The SW air-exposed fish had significantly more NKA cells in the skin than the SW recovery fish (Fig. 3*C*). SW fish had NKA cells significantly larger than those of FW fish (Fig. 3*D*). SW fish in air had cells significantly larger than those of SW fish in water (Fig. 3*D*) or after recovery from air exposure.

Cell Clusters in the Skin

A distinct pattern of cell clusters was observed on the skin surface of all fish (FW and SW, water- and air-exposed), but the pattern was more distinct in SW fish (Fig. 4*A*). Clusters were initially quantified by counting the number of cells in 25 side-by-side grids measuring 50 μm × 50 μm. A clear peak-and-valley pattern was apparent (Fig. 4*B*).

For fish in water, the area of the clusters was significantly greater at site 1 (directly between the pectoral fins) than at site 2 (posterior to site 1; Table 1). The distance between clusters was similar in all sites (Table 1). Also, there were significantly more cells at site 1 that at sites 2 and 3 (4 mm posterior from site 1; Table 1). The area of the clusters was significantly higher at site 1 than at site 3 in air-exposed fish and at site 1 than at sites 2 and 3 in recovery fish (Table 1). As well, the number of cells was lower and the distance between clusters was higher at site 3 relative to site 1 in recovery fish (Table 1). In all cases, the differences between sites were relatively small (22%–37%).

At site 1, recovery fish had significantly smaller distances between the clusters than fish in water and in air (Table 1). Similarly, at site 2, the recovery fish had distances between the clusters that were significantly smaller than those for fish in water but not those of air-exposed fish (Table 1). At site 3, the areas of the clusters in recovery fish were significantly smaller than those of fish in water (control fish; Table 1). The mean number of cells per cluster (20–30) was not significantly different for any of the groups at any of the sites.

Number of Ionocytes in the Skin versus the Gills

The estimated total number of ionocytes in the whole skin was similar to that in the whole gills, but significant differences were found ($FW_{skin} < FW_{gills}$ and $SW_{skin} > SW_{gills}$; Fig. 5). The SW fish had significantly more skin and less gill cells than FW fish (Fig. 5). Within salinities, the FW air-exposed fish had significantly more cells in the skin and gills than the water-exposed groups (Fig. 5). As well, the FW recovery fish had significantly fewer cells in the skin and gills than the air-exposed

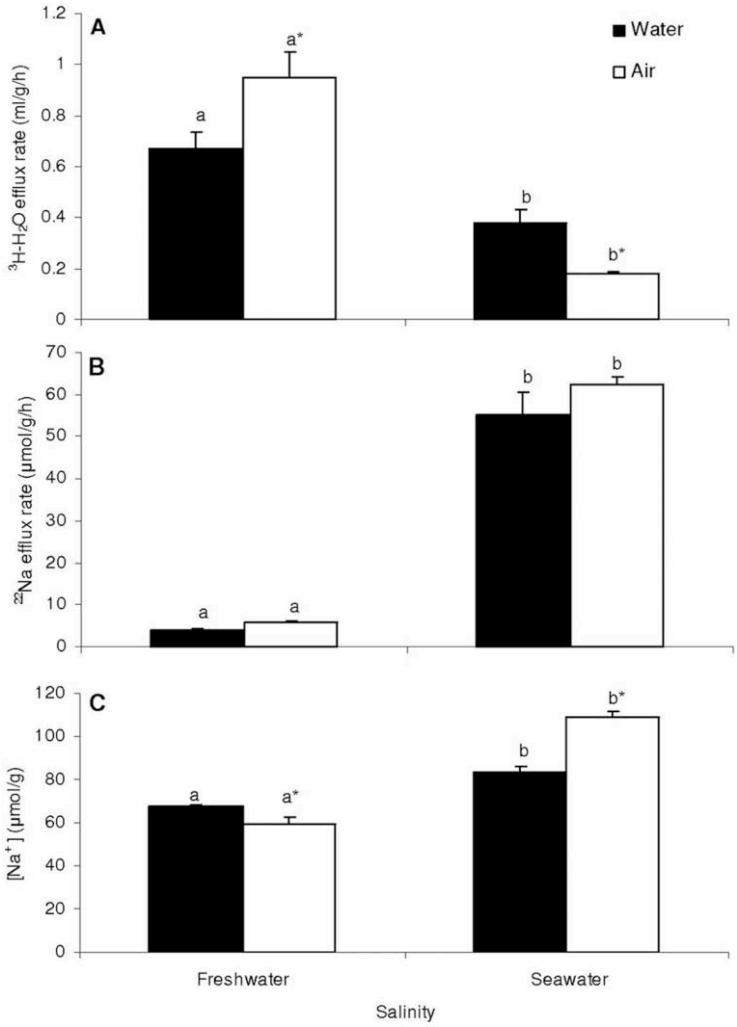

Figure 1. ^{3}H-H_2O (*A*) and ^{22}Na (*B*) efflux rates and whole-body Na^+ concentrations (*C*) of freshwater (FW)- and saltwater (SW)-acclimated *Kryptolebias marmoratus* in water (*black bars*) and in air (*white bars*). Significant differences ($P < 0.05$) between FW- and SW-acclimated fish within a group are marked with different letters. An asterisk denotes significant differences ($P < 0.05$) between water-exposed and air-exposed groups of fish within either FW- or SW-acclimated fish. Values are means ($N = 8$–11) ± SEM.

groups. In SW fish, the recovery fish had significantly fewer cells in the skin than the air-exposed groups (Fig. 5).

Mucous Cells (PAS Staining) in the Skin

There were significantly more (threefold) skin mucous cells in FW air-exposed fish than in the SW air-exposed fish (Fig. 6*A*). There were significantly fewer cells in the FW recovery group than in the FW air-exposed fish (Fig. 6*A*). In the SW group, the number of mucous cells varied significantly ($SW_{water} > SW_{recovery} > SW_{air}$; Fig. 6*A*). The SW recovery fish had significantly larger mucous cells than the FW recovery fish and SW air-exposed fish (Fig. 6*B*).

In terms of the mucous cells, in all groups except the air-exposed SW fish, the ventral section had more cells than the dorsal and left and right lateral sections (Table 2). Also, in FW air-exposed fish and SW water-exposed and recovery fish, the dorsal section had more cells than the two lateral sections (Table 2). In all sections, FW air-exposed fish had more cells than SW air-exposed fish (Table 2). There were too few mucous cells in the gills to quantify.

NKA-Rich Cells in the Gills

NKA-rich cells were found mostly on the gill filaments of fish in water (Fig. 7*A*, 7*B*), but this was not apparent in air-exposed fish because an ILCM obliterated the lamellar-filamental boundaries (Fig. 7*C*, 7*D*). Only a few of the NKA cells were observed near the edge of the gill structure close to the external environment in air-exposed fish, but many NKA cells were embedded within the clublike gill (Fig. 7*C*, 7*D*). In all groups, the number of NKA cells was greater in FW fish than in SW fish (Fig. 7*E*). In FW, the number of NKA cells was greater in air-exposed fish than in water-exposed and recovery fish (Fig. 7*E*).

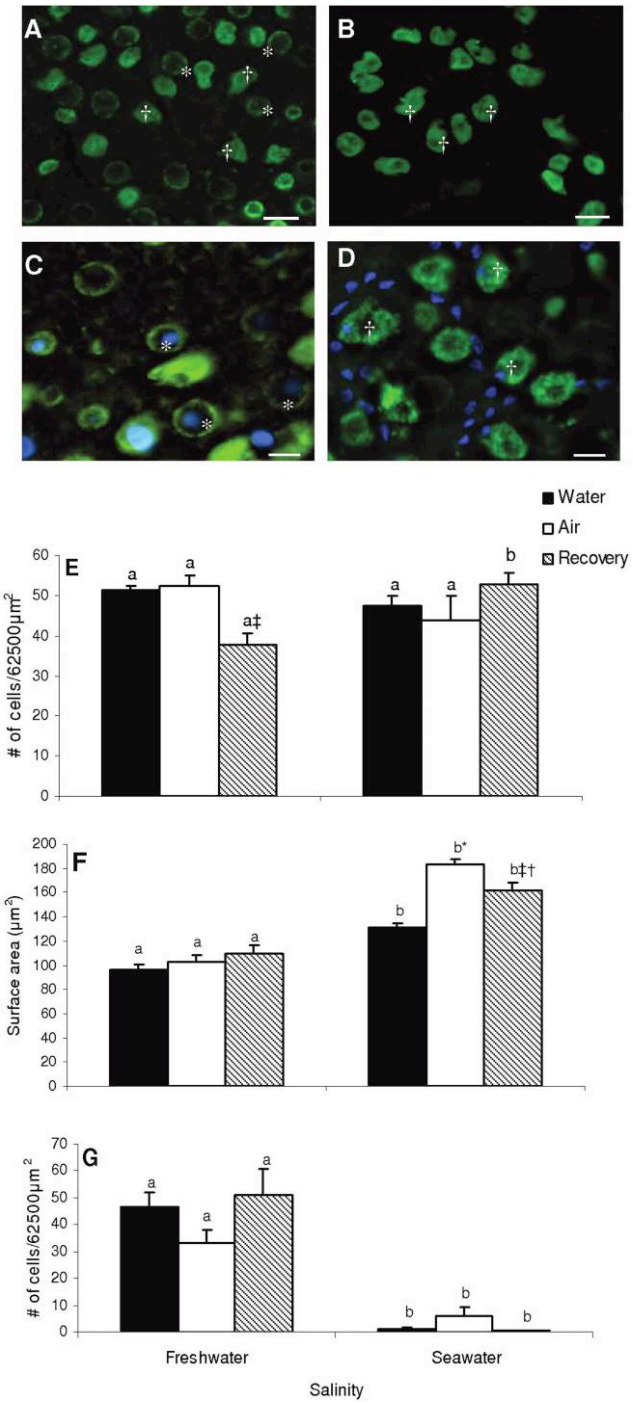

Figure 2. Representative images of 2-(4-dimethylaminostyryl)-1-ethylpyridinium iodide (DASPEI)-stained mitochondria-rich cells (MRCs) in the skin of *Kryptolebias marmoratus* acclimated to freshwater (FW; *A*) or saltwater (SW; *B*). An asterisk indicates a round MRC (stained at edges and having a "doughnut" appearance); a dagger indicates an oval MRC (more strongly and uniformly stained). These images are from fish in water. Scale bars = 20 μm. Also, in *C* and *D*, there are representative images of double-labeled MRCs in the skin of *K. marmoratus* (acclimated to brackish water, 15‰). Cells were stained with DASPEI to label mitochondria (*green*) and with 4′, 6-diamidino-2-phenylindole (DAPI) to label DNA in the nuclei (*blue*). *C*, Nuclei appearing in the round MRCs (*asterisks*). *D*, Nuclei appearing in oval MRCs (*dagger*). Scale bars = 10 μm. The graphs depict the average number (*E*) and cross-sectional area (*F*) of DASPEI-stained oval MRCs or the cross-sectional area (*G*) of DASPEI-stained round MRCs in 0.0625-mm² grids on the ventral skin surface of FW- and SW-acclimated *K. marmoratus* in water (*black bars*), in air (*white bars*), and in the recovery treatment (*hatched bars*). Significant differences ($P < 0.05$) between FW- and SW-acclimated fish within a group are marked with different letters. An asterisk denotes a significant difference ($P < 0.05$) between the water- and air-exposed groups; a dagger denotes a significant difference from the air group; a double dagger denotes a significant difference ($P < 0.05$) between the recovery group and the other two groups. Values are means ($N = 5–8$) ± SEM.

In all groups, the cross-sectional area of the NKA cells was significantly larger in the SW fish than in the FW fish (Fig. 7*F*). FW air-exposed fish had significantly larger NKA cells than the FW fish in the water-exposed group but not the recovery group (Fig. 7*F*).

Gill Morphometrics

There were no significant differences in average lamellar height ($FW_{water} = 46.8 \pm 2.9$ μm, $FW_{air} = 42.5 \pm 2.3$ μm, $FW_{recovery} = 47.2 \pm 2.6$ μm, $SW_{water} = 53.5 \pm 3.9$ μm, $SW_{air} = 45.5 \pm 2.0$ μm, $SW_{recovery} = 46.4 \pm 3.0$ μm) or average lamellar width ($FW_{water} = 7.1 \pm 0.3$ μm, $FW_{air} = 6.4 \pm 0.5$ μm, $FW_{recovery} = 7.0 \pm 0.5$ μm, $SW_{water} = 7.0 \pm 0.3$ μm, $SW_{air} = 6.5 \pm 0.3$ μm, $SW_{recovery} = 7.1 \pm 0.4$ μm) between any of the fish. The ILCM height of SW fish in water was significantly smaller (33%) than that of FW fish in water (Fig. 8). There was a significant increase in the ILCM height with air exposure (relative to that of the fish in water) in both FW (23%) and SW (67%) fish (Fig. 8). These changes were reversible, with a return to control values in the recovery fish.

Discussion

In this study, we have shown that *Kryptolebias marmoratus* survives for at least 9 d out of water in contact with a low- (1‰) or a high-salinity (45‰) moist surface. Radiolabeled ions and water were exchanged across the skin at rates that were not greatly different from those in water-exposed fish. Homeostasis of whole-body Cl^- and H_2O levels was maintained in emersed fish, whereas Na^+ homeostasis was moderately disturbed. Using a mitochondrial marker (DASPEI) and an NKA antibody, we showed that ionocytes were present in both skin and gills under all conditions (FW and SW, water and air exposure) and that skin ionocyte cross-sectional area increased in air-exposed (SW) fish. The gross morphology of the gill was reversibly altered in emersed fish, and ionocytes were not consistently observed on the external surface. The whole cutaneous surface had a similar number of ionocytes relative to the whole gills, and skin cells were arranged in a cluster pattern. Taken together, these results provide evidence that the skin is a site of ion and water exchange and that when *K. marmoratus* are out of water, the skin probably plays a more prominent role in osmoregulation than the gills.

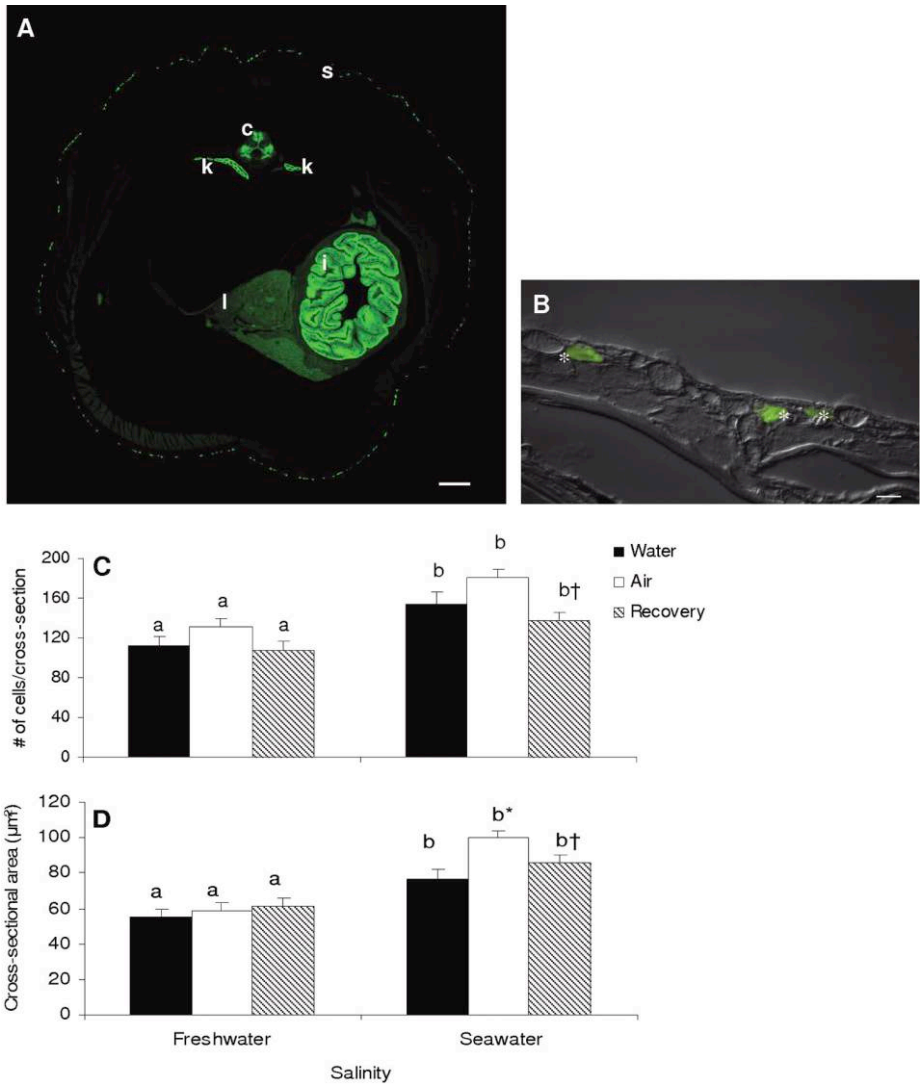

Figure 3. Representative images of immunohistochemically stained cross-sections of the skin in saltwater (SW)-acclimated *Kryptolebias marmoratus* in water. *A*, Whole-body cross-section (scale bar = 100 μm) showing the skin (*s*). The spinal column (*c*), liver (*l*), kidney (*k*) and gut (*i*) likely fluoresce because there are high levels of Na^+, K^+-ATPase (NKA) in those tissues (Clendenon et al. 1978; Fuentes et al. 1997; Sherwani and Parwez 2008). *B*, Section of the skin at a higher magnification (scale bar = 10 μm); NKA-labeled cells are indicated with asterisks. Tissue is oriented so that the external skin surface is at the top. *C*, Total number of NKA cells in cross-sections of the skin of FW- and SW-acclimated *K. marmoratus* in water (*black bars*), in air (*white bars*), and in the recovery treatments (*hatched bars*). A dagger denotes a significant decrease ($P < 0.05$) in the cross-sectional area and number of cells counted in the SW-acclimated recovery fish compared with the air-exposed fish. Values are means ($N = 3$–8) ± SEM. *D*, Average cross-sectional area of NKA cells in FW- and SW-acclimated fish. An asterisk denotes a significant increase ($P < 0.05$) in the cross-sectional area of the NKA cells in SW-acclimated air-exposed fish compared with the water-exposed group. Values are means ($N = 7$–8) ± SEM. On both graphs, significant differences ($P < 0.05$) between FW- and SW-acclimated fish within a group are marked with different letters.

Experimental Approach

DASPEI staining and immunohistochemistry for NKA were both used as markers for ionocytes in the skin. From the similarity between the cross-sectional area measurements of oval DASPEI-stained and NKA-labeled cells between different experimental regimes, it is likely that we are identifying the same population of ionocytes with both techniques. Cell counts between DASPEI staining and NKA labeling could not be directly compared because cells were counted on entirely different planes (flat skin surface and transverse sections, respectively). Further reference to ionocytes in the skin represents a combination of the data from both techniques, whereas reference to ionocytes in the gills represents NKA-labeled cells. It should be noted that in the skin of FW *K. marmoratus*, there appears to be at least two types of ionocytes (oval and round). Ionocyte

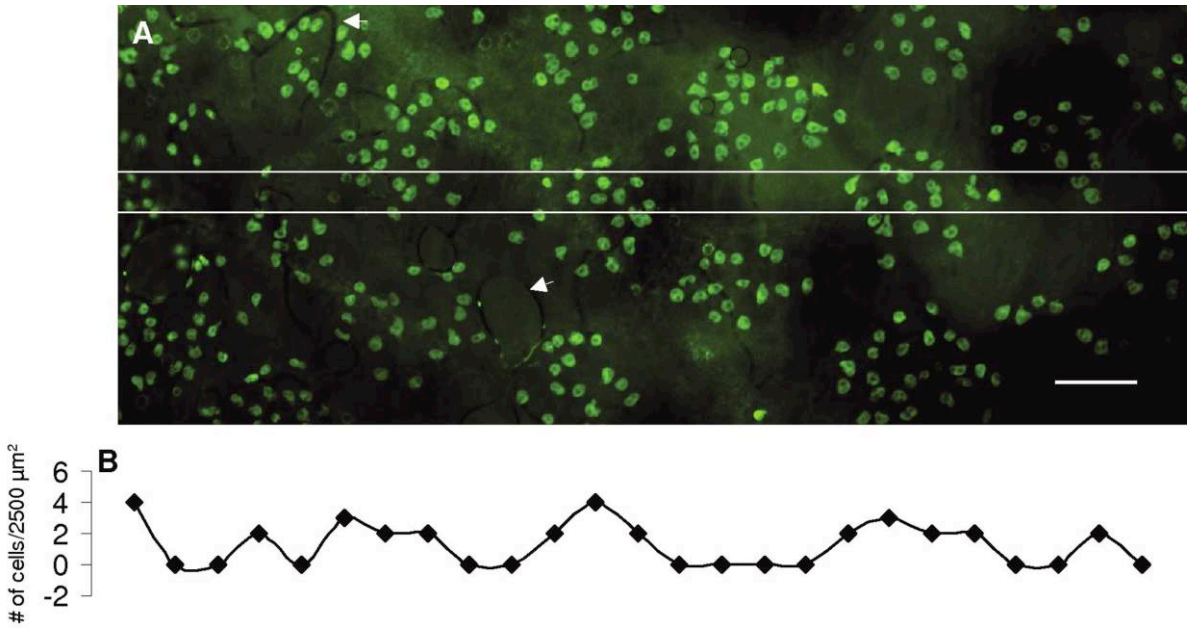

Figure 4. *A*, Representative fluorescent image of cell clustering of mitochondria-rich cells in the ventral skin of SW-acclimated *Kryptolebias marmoratus* in water. This fish was incubated in a 350-μM solution of 2-(4-dimethylaminostyryl)-ethylpyridinium iodide for at least 3 h and then imaged. Blood vessels beneath the skin surface are marked with arrows. *B*, Number of cells per 2,500-μm^2 grid along the section of the image between the white lines (which is 1,250 μm in length). Scale bar = 100 μm.

subtypes have been described in other species (for reviews, see Perry 1997 and Marshall and Grossell 2006), but further histological studies would be required to characterize the properties of these cells in *K. marmoratus*.

In this study, we chose to measure efflux but not influx rates, on the assumption that after 9 d in a treatment, influx and efflux rates should be in approximate equilibrium. In addition, this approach avoided the use of large amounts of expensive ^{22}Na that would be required to measure Na^+ influx in SW fish as well as the need to kill these valuable animals. In the common killifish (*Fundulus heteroclitus*), Na^+ and Cl^- concentrations were measured after fish were transferred from 10% SW to FW and from 10% SW to 100% SW. In most cases, the fish established equilibrium after 7 d, and whole-body Na^+ and Cl^- concentrations were similar to those reported for control fish (Wood and Laurent 2003). Therefore, in this experiment, fish were left in air for 9 d, a period of time that was likely sufficient for influx and efflux to reach equilibrium.

Table 1: Characterization of cell clusters in the ventral skin of mangrove killifish *Kryptolebias marmoratus*

Measurement, Site	Water	Air	Recovery
Area of clusters (μm^2):			
1	28,700 ± 400	25,400 ± 2,300	28,500 ± 1,800
2	19,900 ± 1,500[a]	20,000 ± 1,900	21,400 ± 900[a]
3	23,200 ± 1,400	18,800 ± 1,400[a]	17,900 ± 900[a,b]
Distance between clusters (μm):			
1	44.0 ± 3.7	45.2 ± 3.4	32 ± 1.5[b,c]
2	47.5 ± 2.4	41.9 ± 2.7	34.6 ± 1.9[b]
3	46.8 ± 2.7	45.6 ± 2.7	39.3 ± 2.5
Cells per cluster:			
1	31 ± 2	25 ± 3	28 ± 2
2	22 ± 1[a]	21 ± 3	21 ± 1
3	23 ± 1[a]	19 ± 2	18 ± 2[a]

Note. Characterization of cell clusters collected from sites 1–3 in the ventral skin of saltwater-acclimated mangrove killifish in water, air, and recovery groups. Values are means (N = 7–8) ± SEM.

[a]Significant ($P < 0.05$) difference from site 1.

[b]Significant difference ($P < 0.05$) from the water group.

[c]Significant difference ($P < 0.05$) from the air group.

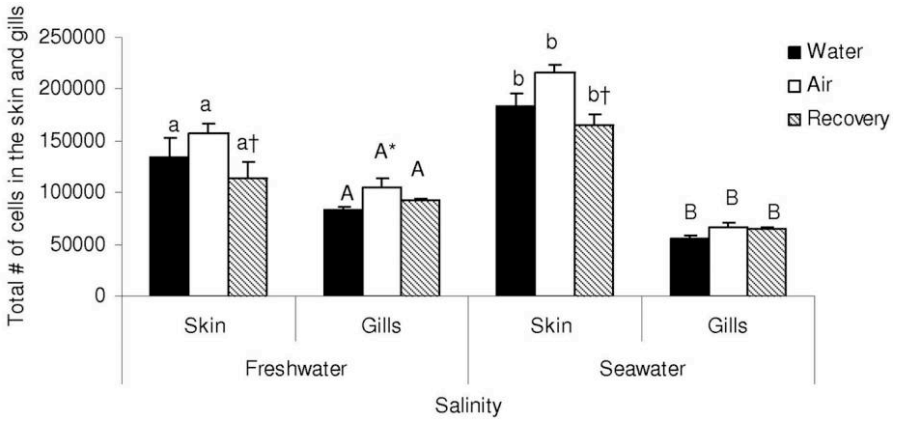

Figure 5. Estimated total number of ionocytes in the skin versus the gills of FW- and SW-acclimated *Kryptolebias marmoratus* in water, in air, and in the recovery treatments. The skin had significantly fewer cells than the gills in FW fish ($P < 0.05$) and more cells than the gills in SW fish ($P < 0.05$). Significant differences ($P < 0.05$) between FW- and SW-acclimated fish within a group are marked with different letters. Significant differences ($P < 0.05$) between FW- and SW-acclimated fish are marked with lowercase (skin) and uppercase (gills) letters. A dagger denotes a significant difference ($P < 0.05$) between the recovery group and the air-exposed groups. An asterisk denotes a significant increase ($P < 0.05$) relative to the water-exposed group. Values are means ($N = 6$–8) ± SEM.

Aquatic Ionoregulation in FW versus SW

Kryptolebias marmoratus are tolerant of a wide range of water salinities (0‰–114‰; King et al. 1989), and their ionoregulatory strategy in FW (1‰) and hypersaline SW (45‰) appears to be similar to that of other euryhaline teleosts. Higher rates of diffusive water exchange in FW relative to SW *K. marmoratus* in water are consistent with data on marine and FW teleosts (e.g., Evans 1969; Motais et al. 1969). In this study, Na^+ efflux rates in SW fish were about 16 times those in their FW counterparts. In previous studies, Na^+ fluxes were consistently higher in SW-acclimated than in FW-acclimated euryhaline teleosts (e.g., Potts and Evans 1967; Forrest et al. 1973; Bath and Eddy 1979; Wood and Laurent 2003). Whole-body Na^+ concentrations in *K. marmoratus* were slightly but significantly higher in SW fish than in FW fish in water, whereas Cl^- concentrations were approximately the same. Whole-body or plasma ion concentrations in euryhaline species transferred to a different water salinity typically show acute changes followed by stabilized values (e.g., Wood and Laurent 2003; Mackie et al. 2005). It is unlikely that intracellular amino acids contributed to tissue osmoregulation, because in a previous study, whole-body total free amino acid levels did not change in *K. marmoratus* transferred from water of 15‰ salinity to 0‰ or 45‰ water (Frick and Wright 2002*a*).

On the whole, skin and gill ionocytes were larger in SW than in FW *K. marmoratus* in water. Gill ionocytes that are larger in SW-acclimated than in FW-acclimated fish have been reported in tilapia (*Oreochromis mossambicus*; Uchida et al. 2000) and Hawaiian gobies (*Stenogobius hawaiiensis*; McCormick et al. 2003) as well as in *K. marmoratus* (King et al. 1989). Interestingly, the number of gill ionocytes was lower in SW than in FW *K. marmoratus* in water. Similar changes in gill MRCs (increased size and decreased density in SW-acclimated relative to FW-acclimated fish) were noted in tilapia *Oreochromis mossambicus* (van der Heijden et al. 1997). Multiplying cell density by cell size provides a rough estimation of the space occupied by MRCs in SW- and FW-acclimated fish (van der Heijden et al. 1997), and in *K. marmoratus* these calculations reveal that very little change (<7%) occurred in the relative occupation of gill NKA-positive cells between the two salinities.

One noteworthy difference between the FW- and SW-acclimated fish in water was that the ILCM height was significantly greater in the FW-acclimated than in the SW-acclimated fish. Fish that develop a gill ILCM in higher-oxygen/lower-temperature FW environments (Sollid et al. 2003, 2005; Nilsson 2007; Matey et al. 2009; Mitrovic and Perry 2009) are thought to be balancing the oxygen requirement against the loss of blood ions (osmorespiratory compromise; Gonzalez and McDonald 1992). The differences in ILCM height with salinity in this study suggests that gill remodeling in *K. marmoratus* occurs in response to both air exposure (Ong et al. 2007) and blood-to-water ion gradients.

Role of Skin versus Gill under Terrestrial Conditions

We hypothesized that the skin plays a role in osmo- and ionoregulation in *K. marmoratus* in water and air. Ionocytes were discovered in the skin of FW and SW fish under all conditions, and the estimated number of cells over the whole skin was comparable to the gills. In embryonic and larval fishes that respire cutaneously, ionocytes are mostly present in the skin, but over developmental time, the number of ionocytes in the skin decreases, whereas the number increases in the gills (Fu et al. 2010; see reviews by Varsamos et al. 2005; Rombough 2007). In the estuarine mudskipper *Periophthalamus modestus*, DASPEI-positive cells were found in the epidermis behind the

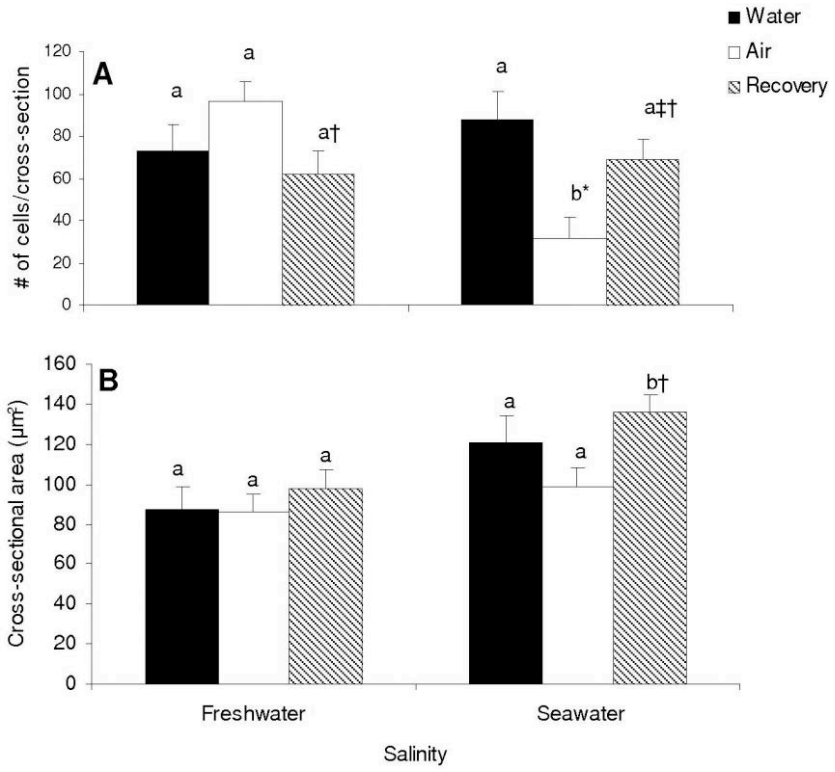

Figure 6. Total number (*A*) and average cross-sectional area (*B*) of mucous cells in the skin of FW- and SW-acclimated *Kryptolebias marmoratus* in water (*black bars*), in air (*white bars*), and in the recovery treatments (*hatched bars*). Significant differences ($P < 0.05$) between FW- and SW-acclimated fish within a group are marked with different letters. An asterisk denotes a significant difference ($P < 0.05$) between water- and air-exposed fish, a double dagger denotes a significant difference ($P < 0.05$) between water-exposed and recovery fish, and a dagger denotes a significant difference ($P < 0.05$) between air-exposed and recovery fish. Values are means (*A*: $N = 4$–8; *B*: $N = 2$–8) ± SEM.

pectoral fin at densities (~1,000 mm^{-2}) similar to those in this study (~1,200 mm^{-2}). Ionocytes were also identified in the skin of *Periophthalamus cantonensis* but not in that of the mudskipper *Boleophthalmus pectinirostris* (Yokoya and Tamura 1992). After transfer to SW, ionocytes appear in the abdominal epidermis of the guppy *Poecilia reticulata* (Schwerdtfeger and Bereiter-Hahn 1978). Thus, skin ionocytes occur in a number of species, but changes in cell size and density with aerial exposure in an amphibious fish have not been previously reported. These results suggest that the skin ionocytes in *K. marmoratus* play an important role in ionoregulation in air.

If the skin plays a role in osmoregulation, then water and

Table 2: Mucous cell counts in cross-sections of skin in the mangrove killifish *Kryptolebias marmoratus*

	Freshwater Acclimated			Seawater Acclimated		
Section	Water	Air	Recovery	Water	Air	Recovery
Dorsal	16 ± 4	27 ± 4[a]	11 ± 4	22 ± 4[a]	11 ± 4[b]	21 ± 3[a]
Ventral	41 ± 7[c]	44 ± 5[c]	39 ± 6[c]	51 ± 6[c]	14 ± 5[b]	37 ± 5[c]
Left lateral	8 ± 3	13 ± 3	7 ± 3	6 ± 3	3 ± 3[b]	6 ± 2
Right lateral	9 ± 3	12 ± 2	4 ± 3	9 ± 2	4 ± 2[b]	6 ± 2

Note. Mucous cell counts in the skin from freshwater (FW)- and saltwater (SW)-acclimated mangrove killifish in water, air, and recovery groups. Values are means ($N = 4$–8) ± SEM.

[a]The dorsal section (within group and salinity) had significantly ($P < 0.05$) more cells than the left and right lateral sections.

[b]Within sections and group, all the sections in the FW-acclimated air-exposed fish had significantly more ($P < 0.05$) mucous cells than all the sections in SW-acclimated air-exposed fish.

[c]The ventral section (within group and salinity) had significantly ($P < 0.05$) more cells than all the other sections.

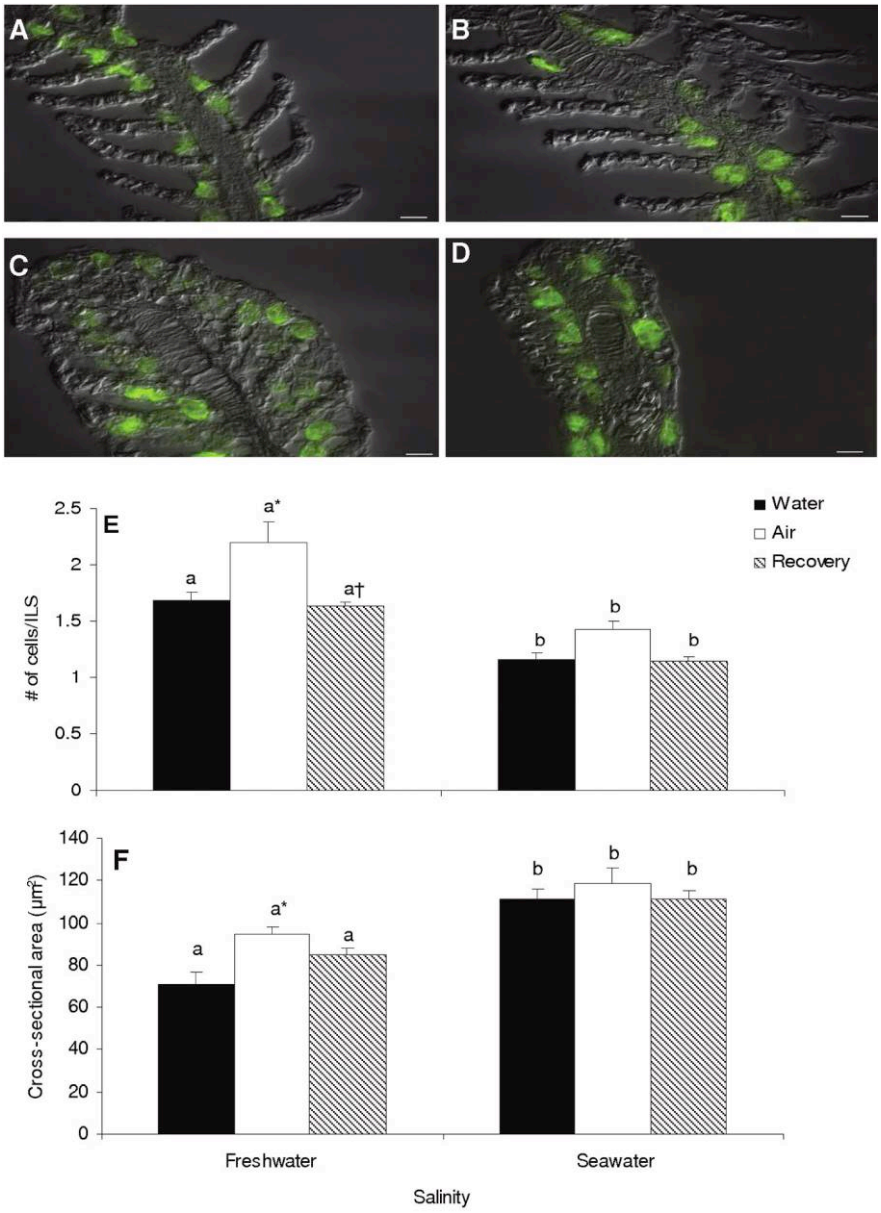

Figure 7. Representative images of immunohistochemically stained gills of freshwater (FW)-acclimated (*A*, *C*) and saltwater (SW)-acclimated (*B*, *D*) *Kryptolebias marmoratus* in water (*A*, *B*) and in air (*C*, *D*). Na^+, K^+-ATPase (NKA) cells appear green. Note that there are more NKA cells in the interlamellar space (ILS) on the filament of FW-acclimated fish than in that of SW-acclimated fish and that NKA cells appear larger in SW-acclimated fish than in FW-acclimated fish. Scale bars = 10 μm. The graphs depict the average number (*E*) and cross-sectional area (*F*) of NKA-labeled cells (in the gills) per ILS in FW- and SW-acclimated *K. marmoratus* in water (*black bars*), in air (*white bars*), and in the recovery treatments (*hatched bars*). Significant differences ($P < 0.05$) between FW- and SW-acclimated fish within a group are marked with different letters. An asterisk denotes a significant increase ($P < 0.05$) in the number and cross-sectional area of NKA-labeled cells per ILS in the FW-acclimated air-exposed fish compared with the water-exposed fish. A dagger denotes a significant decrease ($P < 0.05$) in the number of NKA-labeled cells per ILS in the FW-acclimated recovery fish relative to air-exposed fish. Values are means ($N = 6$–8) ± SEM.

ion flux should occur across the skin, and this was indeed the case. When air-exposed killifish were placed in a mesh-bottomed chamber in contact with a pool of water containing radioisotopes, they absorbed the radioisotopes. This was first demonstrated by the appearance of ^{22}Na and ^{3}H-H_2O counts in air-exposed fish in contact with the radioisotopically labeled water. When these fish were then placed on a mesh surface over clean water (without radioisotopes), ^{22}Na and ^{3}H-H_2O appeared in the water. The transfer of radioisotopes likely occurred mostly across the skin because the gills were not in direct contact with water. However, we cannot completely rule out gill air/water exchange because water may have entered the

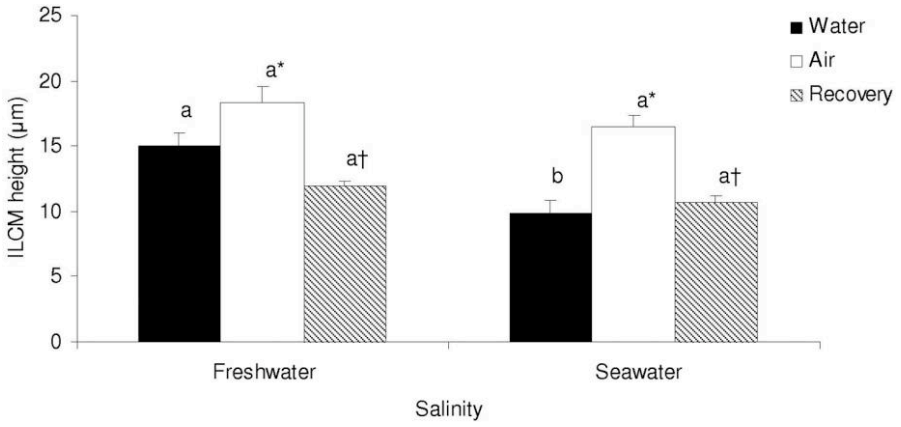

Figure 8. Interlamellar cell mass (ILCM) height measured in the gills of FW- and SW-acclimated *Kryptolebias marmoratus* in water (*black bars*), in air (*white bars*), and in the recovery treatments (*hatched bars*). Significant differences ($P < 0.05$) between FW- and SW-acclimated fish within a group are marked with different letters. An asterisk denotes a significant increase in the ILCM height in air-exposed fish compared with water-exposed fish. A dagger denotes a significant decrease in the ILCM height in recovery fish compared with air-exposed fish. Values are means ($N = 6–8$) ± SEM.

opercular chamber through capillary action (see below). These ion flux results, as well as the presence and regulation of skin ionocyte morphometrics, support the hypothesis that the skin is involved in osmo- and ionoregulation in *K. marmoratus*.

We predicted that during air exposure, the gills (if functional) would have a reduced role in exchange with the external environment. Indeed, the lamellar surface area of the gills decreased because of an increase of the ILCM height in air-exposed *K. marmoratus* in both salinities. Ong et al. (2007) hypothesized that an ILCM develops during emersion in *K. marmoratus* to support the gills and prevent collapse and possibly to limit desiccation by reducing gill surface area. In this study, gill ionocytes were observed along the filamental surface between lamellae in both FW and SW fish in water, but in emersed fish they were scattered throughout the clublike gill structure. This contrasts with findings in *Arapaima gigas* and *Carassius auratus*, where gill remodeling involves a reorientation of gill ionocytes to the outside edge of the embedded lamellae (Brauner et al. 2004; Mitrovic and Perry 2009).

If the gill has a reduced role in osmoregulation during air exposure, then the number or size of ionocytes in the gills might be expected to decrease. In the gills of FW air-exposed killifish, surprisingly, there was an increase in the number and size of ionocytes relative to killifish in water, and this was reversed in the recovery group. The physiological significance of these changes in the FW gill is unknown. Fish in our experiments had no opportunity to gulp water when in aerial conditions, and to our knowledge, there are no reports in the literature of this behavior, but it has been observed in amphibious mudskippers, *P. cantonensis* (Gordon et al. 1978) and *Periophthalamus schlosseri* (Chew et al. 2007). It is still possible, however, that the gills have access to water in some terrestrial habitats. In this study, capillary action created by the porous mesh (below air-exposed fish) may have drawn water up into contact with the operculum, where it might have been further wicked into the opercular cavity. Therefore, we cannot rule out the possible involvement of gill ionocytes in ion exchange even when there was no significant water flow over the gills.

In fish stained with DASPEI, clusters of MRCs were observed in the skin of both SW and FW fish. The cell-cluster pattern was not altered in air-exposed fish. Sturla et al. (2001) observed MRC clusters of about three to five cells in the opercular skin of FW African lungfish (*Protopterus annectens*), whereas cell clustering (two or three cells) occurs in SW- but not FW-acclimated Japanese eel (*Anguilla japonica*) during early life stages (Sasai et al. 1998). Interestingly, in the mangrove killifish, the cell clusters were much larger (20–30 cells). It has been proposed that these cell clusters are important for sodium extrusion in the eel (Sasai et al. 1998). Epidermal ionocyte clustering in zebrafish embryos is regulated by Delta/Jagged-Notch signaling, and a loss of signaling leads to a higher density of ionocytes in clusters (Hsiao et al. 2007; Jänicke et al. 2007). More work is necessary to understand the functional role of these skin ionocyte clusters in *K. marmoratus*.

In air, total body water and Na^+ exchange rates might be expected to decrease because of decreased gill surface area for exchange in the fish, all else being equal. Decreased diffusive water exchange rates observed in air-exposed SW fish were possibly due to reduced passive water loss to the environment because the surface area for exchange was reduced. However, water exchange increased in air-exposed FW fish, opposite to our predictions and previous data on air-exposed FW African lungfish *Protopterus dolloi* (Wilkie et al. 2007). Water permeability of epithelial barriers (epidermis, branchial, renal) is regulated by numerous factors, including tight-junction proteins (Bagherie-Lachidan et al. 2008) and aquaporins (Agre et al. 1995; Cutler and Cramb 2000). Expression of these proteins may have been altered in air-exposed fish, resulting in modified water efflux rates, but whether this occurred is unknown. It is unlikely that fish lost a significant amount of water by evap-

oration because the relative humidity was at least 99% in the experimental chambers during air exposure (D. LeBlanc, unpublished data), and body water content did not change.

As predicted, air-exposed *K. marmoratus* largely maintained ionoregulatory and osmoregulatory homeostasis; however, whole-body Na^+ concentrations in FW were slightly but significantly lower, while in SW they were significantly higher, relative to control fish in water. The direction of these changes follows the passive gain of NaCl in SW and passive loss in FW. The turnover time of the internal Na pool, estimated by dividing the measured whole-body Na concentration (× 0.95) by the measured efflux rates, is about 12 h in FW fish and 1.5 h in SW fish. It is therefore very unlikely that the fish are much out of equilibrium by 9 d (216 h = 18 turnover times in FW, 144 turnover times in SW). Influx and efflux rates are probably back in balance, but the internal body Na pool has been reset to a higher or lower level. When *Synbranchus marmoratus* (~1‰) and *P. schlosseri* (~8‰) were emersed, Na^+ (influx and efflux) and Ca^{2+} (influx), respectively, continued to move through the skin (Stiffler et al. 1986; Fenwick and Lam 1988). It is unlikely that the kidney was involved in Na^+ efflux in SW fish to any great extent because mostly divalent ions and few monovalent ions are released in urine (Marshall and Grosell 2006). Therefore, it is likely that air-exposed killifish primarily use ionocytes in the skin for active Na^+ efflux in SW but that they have some difficulties maintaining Na^+ balance. In FW fish, we cannot rule out some loss of Na^+ via the urine; however, from studies in other species, this is probably a small component (Curtis and Wood 1991; Marshall and Grosell 2006). Indeed, even in two species of African lungfish (*P. dolloi* and *P. annectens*) that have greatly reduced gills and low skin permeability, measured renal Na^+ loss rates were only 12%–22% of loss rates across the body surface (Patel et al. 2009) in FW.

Whole-body Na^+ concentrations increased to levels substantially higher than whole-body Cl^- concentrations in SW fish in air. We can only speculate that either a compensating cation (anion) decreased (increased) to maintain electrical neutrality. It is possible that whole-body concentrations of K^+ fell in response to rising Na^+. The most likely explanation, however, is that the anion HCO_3^- increased in concentration. We speculate that the fish suffered a respiratory acidosis (CO_2 retention) in air that was metabolically compensated after 9 d by the accumulation of HCO_3^-, a well-documented phenomenon tha occurs when other amphibious fish are transferred to air (e.g., Graham 2006). However, it is not clear why the same Na^+ versus Cl^- discrepancy was not seen in FW killifish exposed t air. This warrants further investigation.

We predicted that during air exposure there would be an increase in the number of mucous cells in the skin and gills, regardless of salinity. However, few mucous cells were found in the gills of FW and SW killifish compared with those reported in some species (Mattheij and Stroband 1971; Gona 1979; Solanki and Benjamin 1982). SW fish in air had significantly fewer mucous cells in the skin relative to the control and recovery groups, the opposite of what would be predicted if mucus production during air exposure helped to limit des iccation or facilitated ionoregulation. Overall, the results indicate that mucus production is no more important in terrestrial than in aquatic environments.

In conclusion, we found evidence that the skin of *K. marmoratus* is a site of iono- and osmoregulation in aquatic and terrestrial habitats. We estimated that the cutaneous surface had a number of ionocytes similar to that in the gills and that skin cells were arranged in a cluster pattern of 25–30 cells per cluster. During extended terrestrial periods, gill and skin cells and morphology were reversibly remodeled. *Kryptolebias marmoratus* maintains water balance but not perfect ionic homeostasis during extended terrestrial excursions. These findings provide the first detailed study of iono- and osmoregulation in a cutaneous breathing euryhaline amphibious fish.

Acknowledgments

We would like to thank Linda Diao, McMaster University, for her technical assistance with the radioisotope work; the animal health laboratory and Dr. John Lumsden, University of Guelph, for assistance with histology; Meghan Mitchell and Andrew Russo for fish husbandry; and Lori Ferguson for typographical assistance. We would also like to thank Dr. Jonathan Wilson, Centro Interdisciplinar de Investigação Marinha e Ambiental, Portugal, for helpful comments concerning immunohistochemistry and Dr. Nick Bernier, University of Guelph, for helpful discussions of the data. The α-5 antibody (mouse anti-chicken NKA) developed by D. M. Fambrough (Johns Hopkins University, Baltimore) was obtained from the Developmental Studies Hybridoma Bank developed under the auspices of the National Institute of Child Health and Human Development and maintained by the University of Iowa, Department of Biological Sciences, Iowa City. This project was funded by National Sciences and Engineering Research Council of Canada grants to P.A.W. and C.M.W. C.M.W. is supported by the Canada Research Chair Program. All experiments were approved by the University of Guelph Animal Care Committee.

Literature Cited

Abel D.C., C. Koenig, and W.P. Davis. 1987. Emersion in the mangrove forest fish *Rivulus marmoratus*: a unique response to hydrogen sulfide. Environ Biol Fish 18:67–72.

Agre P., D. Brown, and S. Nielsen. 1995. Aquaporin water channels: unanswered questions and unresolved controversies. Curr Opin Cell Biol 7:472–483.

Bagherie-Lachidan M., S.I. Wright, and S.P. Kelly. 2008. Claudin-3 tight junction proteins in *Tetraodon nigroviridis*: cloning, tissue-specific expression and a role in hydromineral balance. Am J Physiol 294:R1638–R1647.

Bath R.N. and F.B. Eddy. 1979. Salt and water balance in rainbow trout (*Salmo gairdneri*) rapidly transferred from fresh water to sea water. J Exp Biol 83:193–202.

Bereiter-Hahn J. 1976. Dimethylaminostyrylmethylpyridini-

umiodine (DASPMI) as a fluorescent probe for mitochondria in situ. Biochim Biophys Acta 423:1–14.

Brauner C.J., V. Matey, J.M. Wilson, N.J. Bernier, and A.L. Val. 2004. Transition in organ function during the evolution of air-breathing: insights from *Arapaima gigas*, an obligate air breathing teleost from the Amazon. J Exp Biol 207:1433–1438.

Chew S.F., M.Y. Sim, Z.C. Phua, W.P. Wong, and Y.K. Ip. 2007. Active ammonia excretion in the giant mudskipper, *Periophthalmodon schlosseri* (Pallas), during emersion. J Exp Zool 307:357–369.

Clendenon N.R., N. Allen, W.A. Gordon, and W.G. Bingham Jr. 1978. Inhibition of Na^+-K^+-activated ATPase activity following experimental spinal cord trauma. J Neurosurg 49 563–568.

Curtis B.J. and C.M. Wood. 1991. The function of the urinary bladder in vivo in the freshwater rainbow trout. J Exp Biol 155:567–583.

Cutler C.P. and G. Cramb. 2000. Water transport and aquaporin expression in fish. Pp. 433–441 in S. Hohmann and S. Neilsen, eds. Molecular Biology and Physiology of Water and Solute Transport. Kluwer Academic/Plenum, New York.

Davis W.P., D.S. Taylor, and B.J. Turner. 1990. Field observations of the ecology and habits of mangrove rivulus (*Rivulus marmoratus*) in Belize and Florida (Teleostei: Cyprinodontiformes: Rivulidae). Ichthyol Explor Freshw 1:123–134.

Dunson W.A. and D.B. Dunson. 1999. Factors influencing growth and survival of the killifish, *Rivulus marmoratus*, held inside enclosures in mangrove swamps. Copeia 1991:661-668.

Evans D.H. 1969. Studies on the permeability to water of selected marine, freshwater and euryhaline teleosts. J Exp Biol 50:689–703.

Evans D.H., P.M. Piermarini, and K.P. Choe. 2005. The multifunctional fish gill: dominant site of gas exchange, osmoregulation, acid-base regulation and excretion of nitrogenous waste. Physiol Rev 85:97–177.

Fenwick J.C. and T.J. Lam. 1988. Calcium fluxes in the teleost fish tilapia (*Oreochromis*) in water and in both water and air in the marble goby (*Oxyeleotris*) and the mudskipper (*Periophthalmodon*). Physiol Zool 61:119–125.

Forrest J.N., Jr., A.D. Cohen, D.A. Schon, and F.H. Epstein. 1973. Na transport and Na-K-ATPase in gills during adaptation to seawater: effects of cortisol. Am J Physiol 224:709–713.

Frick N.T. and P.A. Wright. 2002*a*. Nitrogen excretion in the mangrove killifish *Rivulus marmoratus*. I. The influence of environmental salinity and external ammonia. J Exp Biol 205. 79–89.

———. 2002*b*. Nitrogen excretion in the mangrove killifish *Rivulus marmoratus*. II. Significant ammonia volatilization in teleost during air exposure. J Exp Biol 205:91–100.

Fu C., J.M. Wilson, P.J. Rombough, and C. Brauner. 2010. Ions first: Na^+ uptake shifts from the skin to the gills before O_2 uptake in developing rainbow trout, *Oncorhynchus mykiss*. Proc R Soc B 277:1553–1560, doi:10.1098/rspb.2009.1545.

Fuentes J., J.L. Soengas, P. Rey, and E. Rebolledo. 1997. Progressive transfer to seawater enhances intestinal and branchial Na^+-K^+-ATPase activity in non-anadromous rainbow trout. Aquacult Int 5:217–227.

Gona O. 1979. Mucous glycoproteins of teleostean fish: a comparative histochemical study. Histochem J 11:709–718.

Gonzalez R.J. and D.G. McDonald. 1992. The relationship between oxygen consumption and ion loss in a freshwater fish. J Exp Biol 163:317–332.

Gordon M.S., W.W.-S. Ng, and A.Y.-W. Yip. 1978. Aspects of the physiology of terrestrial life in amphibious fishes. III. The Chinese mudskipper, *Periophthalmus cantonensis*. J Exp Biol 72:57–75.

Graham J.B. 1973. Terrestrial life of the amphibious fish *Mnierpes macrocephalus*. Mar Biol 23:83–91.

———. 1997. Air-Breathing Fishes: Evolution, Diversity, and Adaptations. Academic Press, San Diego, CA.

———. 2006. Aquatic and aerial respiration. Pp. 85–117 in D.H. Evans and J.B. Claiborne, eds. The Physiology of Fishes. 3rd ed. CRC, Boca Raton, FL.

Grizzle J.M. and A. Thiyagarajah. 1987. Skin histology of *Rivulus ocellatus marmoratus*: apparent adaptations for aerial respiration. Copeia 1987:237–240.

Hiroi J., T. Kaneko, and M. Tanaka. 1999. *In vivo* sequential changes in chloride cell morphology in the yolk-sac membrane of Mozambique tilapia (*Oreochromis mossambicus*) embryos and larvae during seawater adaptations. J Exp Biol 202:3485–3495.

Hsiao C.-D., M.-S. You, Y.-J. Guh, M. Ma, Y.-J. Jiang, and P.-P. Hwang. 2007. A positive regulatory loop between *foxi3a* and *foxi3b* is essential for specification and differentiation of zebrafish epidermal ionocytes. PLoS ONE 2:e302.

Hughes G.M. and J.S.D. Munshi. 1979. Fine structure of the gills of some Indian air-breathing fishes. J Morphol 160:169–194.

Ishimatsu A., G.K. Iwama, T.B. Bentley, and N. Heisler. 1992. Contribution of the secondary circulatory system to acid-base regulation during hypercapnia in rainbow trout. J Exp Biol 170:43–56.

Jänicke M., T.J. Carney, and M. Hammerschmidt. 2007. Foxi3 transcription factors and Notch signaling control the formation of skin ionocytes from epidermal precursors of the zebrafish embryo. Dev Biol 307:258–271.

Kapuściński J. and W. Szer. 1979. Interactions of 4′, 6-diamidine-2-phenylindole with synthetic polynucleotides. Nucleic Acids Res 6:3519–3534.

King J.A.C., D.C. Abel, and R. DiBona. 1989. Effects of salinity on chloride cells in the euryhaline cyprinodontid fish *Rivulus marmoratus*. Cell Tissue Res 257:367–377.

Litwiller S.L., M.J. O'Donnell, and P.A. Wright. 2006. Rapid increase in the partial pressure of NH_3 on the cutaneous surface of air-exposed mangrove killifish, *Rivulus marmoratus*. J Exp Biol 209:1737–1745.

Mackie P., P.A. Wright, B.D. Glebe, and J.S. Ballantyne. 2005. Osmoregulation and gene expression of Na^+/K^+ ATPase in

families of Atlantic salmon (*Salmo salar*) smolts. Can J Fish Aquat Sci 62:2661–2672.

Marshall W.S. 1977. Transepithelial potential and short-circui current across the isolated skin of *Gillichthys mirabilis* (Teleostei: Gobiidae), acclimated to 5% and 100% seawater. J Comp Physiol 114:157–165.

Marshall W.S. and M. Grosell. 2006. Ion transport, osmoregulation and acid-base balance. Pp. 177–230 in D.H. Evans and J.B. Claiborne, eds. The Physiology of Fishes. 3rd ed. CRC, Boca Raton, FL.

Matey V., J.G. Richards, Y. Wang, C.M. Wood, J. Rogers, R Davies, B.W. Murray, X.-Q. Chen, J. Du, and C.J. Brauner. 2009. The effect of hypoxia on gill morphology and iono regulatory status in the Lake Qinghai scaleless carp, *Gymnocypris prezewalskii*. J Exp Biol 211:1063–1074.

Mattheij J.A.M. and H.W.J. Stroband. 1971. The effects of osmotic experiments and prolactin on the mucous cells in th skin and the ionocytes in the gills of the teleost *Cichlasoma biocellatum*. Z Zellforsch 121:93–101.

McCormick S.D., K. Sundell, B.T. Björnsson, C.L. Brown, and J. Hiroi. 2003. Influence of salinity on the localization of Na^+/K^+-ATPase, $Na^+/K^+/2Cl^-$ cotransporter (NKCC) and CFTR anion channel in chloride cells of the Hawaiian gob (*Stenogobius hawaiiensis*). J Exp Biol 206:4575–4583.

Mitrovic D. and S.F. Perry. 2009. The effects of thermally induced gill remodeling on ionocyte distribution and branchial chloride fluxes in goldfish (*Carassius auratus*). J Exp Bio 212:843–852.

Motais R., J. Isaia, J.C. Rankin, and J. Maetz. 1969. Adaptive changes of the water permeability of the teleostean gill epi thelium in relation to external salinity. J Exp Biol 51:529–546.

Nilsson G.E. 2007. Gill remodeling in fish: a new fashion o an ancient secret? J Exp Biol 210:2403–2409.

Nonnette G., Nonnette L., and Kirsch R. 1979. Chloride cells and chloride exchange in the skin of a seawater teleost, th shanny (*Blennius pholis* L.). Cell Tissue Res 199:387–396.

Ong K., D. Stevens, and P.A. Wright. 2007. Gill morphology of the mangrove killifish (*Kryptolebias marmoratus*) is plastic and changes in response to terrestrial air exposure. J Exp Biol 210:1109–1115.

Patel M., F.I. Iftikar, R.W. Smith, Y.K. Ip, and C.M. Wood. 2009. Water balance and renal function in two species o African lungfish *Protopterus dolloi* and *Protopterus annectens*. Comp Biochem Physiol A 152:149–157.

Perry S.F. 1997. The chloride cell: structure and function ir the gills of freshwater fishes. Annu Rev Physiol 59:325–347.

Perry S.F. and Wood C.M. 1985. Kinetics of branchial calcium uptake in the rainbow trout: effects of acclimation to various external calcium levels. J Exp Biol 116:411–433.

Potts W.T.W. and D.H. Evans. 1967. Sodium and chloride balance in the killifish *Fundus heteroclitus*. Biol Bull 133:411–425.

Randall D.J., J.M. Wilson, K.W. Peng, T.K.W. Kok, S.S.L. Kuah, S.F. Chew, T.J. Lam, and Y.K. Ip. 1999. The mudskipper, *Periophthalmodon schlosseri*, actively transports NH_4^+ against a concentration gradient. Am J Physiol 277:R1562–R1567.

Rombough P. 2007. The functional ontogeny of the teleost gill: which comes first, gas or ion exchange? Comp Biochem Physiol A 148:732–742.

Sasai S., T. Kaneko, and K. Tsukamoto. 1998. Extrabranchial chloride cells in early life stages of the Japanese eel, *Anguilla japonica*. Ichthyol Res 45:95–98.

Sayer M.D.J. 2005. Adaptations of amphibious fish for surviving life out of water. Fish Fish 6:186–211.

Sayer M.D.J. and J. Davenport. 1991. Amphibious fish: why do they leave water? Rev Fish Biol Fish 1:159–181.

Schwerdtfeger W.K. and J. Bereiter-Hahn. 1978. Transient occurrence of chloride cells in the abdominal epidermis of the guppy, *Poecilia reticulata* Peters, adapted to sea water. Cell Tissue Res 191:463–471.

Sherwani F.A. and I. Parwez. 2008. Plasma thyroxine and cortisol profiles and gill and kidney Na^+/K^+-ATPase and SDH activities during acclimation of the catfish *Heteropneustes fossilis* (Bloch) to higher salinity, with special reference to the effects of exogenous cortisol on hypo-osmoregulatory ability of the catfish. Zool Sci 25:164–171.

Solanki T.G. and M. Benjamin. 1982. Changes in the mucous cells of the gills, buccal cavity and epidermis of the nine-spined stickleback, *Pungitius pungitius* L., induced by transferring the fish to sea water. J Fish Biol 21:563–575.

Sollid J.D., P. Gundersen. and G.E. Nilsson. 2003. Hypoxia induces adaptive and reversible gross morphological changes in crucian carp gills. J Exp Biol 206:3667–3673.

Sollid J., R.E. Weber, and G.E. Nilsson. 2005. Temperature alters respiratory surface of crucian carp *Carassius carassius* and goldfish *Carassius auratus*. J Exp Biol 208:1109–1116.

Stiffler D.F., J.B. Graham, K.A. Dickson, and W. Stockmann. 1986. Cutaneous ion transport in the freshwater teleost *Synbranchus marmoratus*. Physiol Zool 59:406–418.

Sturla M., M.A. Masini, P. Prato, C. Grattarola, and B. Uva. 2001. Mitochondria-rich cells in gills and skin of an African lungfish, *Protopterus annectens*. Cell Tissue Res 303:351–358.

Taylor S. 1990. Adaptive specializations of the cyprinodont fish *Rivulus marmoratus*. Fla Sci 53:239–248.

———. 2000. Biology and ecology of *Rivulus marmoratus*: new insights and a review. Fla Sci 63:242–255.

Taylor S., B.J. Turner, W.P. Davis, and B.B. Chapman. 2008. A novel terrestrial fish habitat inside emergent logs. Am Nat 171:263–266.

Uchida K., T. Kaneko, H. Miyazaki, S. Hasegawa, and T. Hirano. 2000. Excellent salinity tolerance of Mozambique tilapia (*Oreochromis mossambicus*): elevated chloride cell activity in the branchial and opercular epithelia of the fish adapted to concentrated seawater. Zool Sci 17:149–160.

van der Heijden A.J.H., P.M. Verbost, J. Eygensteyn, J. Li, S.E. Wendelaar Bonga, and G. Flik. 1997. Mitochondria-rich cells in the gills of tilapia (*Oreochromis mossambicus*) adapted to fresh water or sea water: quantification by confocal laser scanning microscopy. J Exp Biol 200:55–64.

Varsamos S., C. Nebel, and G. Charmantier. 2005. Ontogeny of osmoregulation in postembryonic fish: a review. Comp Biochem Physiol A 141:401–429.

Wilkie M.P., T.P. Morgan, F. Galvez, R.W. Smith, M. Kajimura, Y.K. Ip, and C.M. Wood. 2007. The African lungfish (*Protopterus dolloi*): osmoregulation in a fish out of water. Physiol Biochem Zool 80:99–112.

Wood C.M. and P. Laurent. 2003. Na^+ versus Cl^- transport in the intact killifish after rapid salinity transfer. Biochim Biophys Acta 1618:106–119.

Yokoya S. and O.S. Tamura. 1992. Fine structure of the skin of the amphibious fishes, *Boleophthalmus pectinirostris* and *Periophthalmus cantonensis*, with special reference to the location of blood vessels. J Morphol 214:287–297.

Zall D.M., M.D. Fisher, and Q.M. Garner. 1956. Photometric determination of chlorides in water. Anal Chem 28:1665–1678.

Zhang J., T. Taniguchi, T. Takita, and A.B. Ali. 2003. A study on the epidermal structure of *Periophthalmodon* and *Periophthalmus* mudskippers with reference to their terrestrial adaptation. Ichthyol Res 50:310–317.